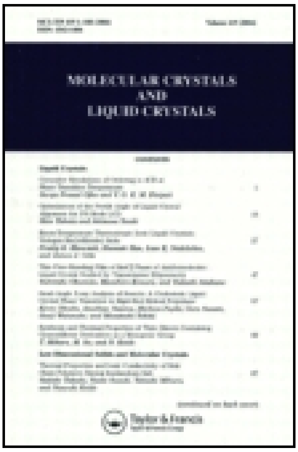

Molecular Crystals and Liquid Crystals
Publication details, including instructions for authors and subscription information:
http://www.tandfonline.com/loi/gmcl20

Surface Plasmon Resonance in Nanostructures Based on Polyparaphenylene - Silver Monolayers

A. D. Zamkovets [a] , A. N. Ponyavina [a] , O. I. Aksimentyeva [b] & L. V. Baran [c]

[a] Institute of Physics, NAS of Belarus, Minsk, Belarus
[b] Ivan Franko Lviv National University of Lviv, Ukraine
[c] Belorussian State University, Minsk, Belarus

Version of record first published: 03 Mar 2011

To cite this article: A. D. Zamkovets, A. N. Ponyavina, O. I. Aksimentyeva & L. V. Baran (2011): Surface Plasmon Resonance in Nanostructures Based on Polyparaphenylene - Silver Monolayers, Molecular Crystals and Liquid Crystals, 536:1, 86/[318]-92/[324]

To link to this article: http://dx.doi.org/10.1080/15421406.2011.538307

Mol. Cryst. Liq. Cryst., Vol. 536: pp. 86/[318]–92/[324], 2011

ISSN: 1542-1406 print/1563-5287 online
DOI: 10.1080/15421406.2011.538307

Surface Plasmon Resonance in Nanostructures Based on Polyparaphenylene – Silver Monolayers

A. D. ZAMKOVETS,[1] A. N. PONYAVINA,[1]
O. I. AKSIMENTYEVA,[2] AND L. V. BARAN[3]

[1]Institute of Physics, NAS of Belarus, Minsk, Belarus
[2]Ivan Franko Lviv National University of Lviv, Ukraine
[3]Belorussian State University, Minsk, Belarus

Spectral and structural properties of two-layered polyparaphenylene-silver nanostructures fabricated by a successive thermal evaporation of appropriate materials in vacuum have been studied. We have established an unusual large long-wave shift of the metal nanoparticle surface plasmon absorption resonance (SPAR) and analyzed the main mechanisms of the shift observed. Together with the Coulomb dynamic screening of collective electron oscillations in a metal nanoparticle by the matrix material, we have also considered an additional mechanism caused by the coupling of polyparaphenylene π- electrons with silver valence electrons.

Keywords Monolayer; optical spectra; polyparaphenylene; silver nanoparticles; surface plasmon resonance

Introduction

In the recent years, there is a growing interest to polymers with a π-conjugated electron system. They have delocalized electron states that hold electroconductivity in a conjunction chain [1]. Activation of the conjugated polymers allows changing their conductivity at a wide range, as well as controlling the width of the band gap. This unique possibility shows a considerable promise for the creation of optoelectronic devices of various functions, among them flat electroluminescent displays, memory systems, photo voltaic cells, etc.

New perspectives are opening at using the conjugated polymers coupled with the noble metal nanoparticles, i.e., the so-called plasmonic nanoparticles, for which the surface plasmon absorption resonances (SPAR) are formed in the visible and near IR ranges [2]. In the SPAR spectral range, plasmonic nanoparticles amplify local fields near their surface, which allows controlling the barrier properties of created coupled systems. Changing the silver particle sizes and/or the surface concentration may shift the SPAR band practically through the whole visible range of the spectrum with a simultaneous shift of the spectral range, where a local field is enhanced. In this

---

Address correspondence to O. I. Aksimentyeva, Ivan Franko Lviv National University of Lviv, Ukraine. E-mail: aksimen@ukr.net

paper, we present the data on the optical and structural properties of two-component systems based on the conducting polymer polyparaphenylene (PPP) and silver nanoparticle monolayers. The PPP/Ag systems were obtained by a successive thermal evaporation of these materials in vacuum on the glass and quartz substrates (S).

Experimental Methods

Nanostructures were fabricated with the use of a vacuum device VU-1A at a residual gas pressure of $(2\text{–}5) \cdot 10^{-5}$ Torr by a successive thermal evaporation of PPP and Ag on the glass or quartz substrates. At the thermal evaporation of a metal on a substrate, the metal island structure (monolayer of nanoparticles) is formed at the first stage. At room temperature of substrates and silver surface density of $(1.3\text{–}5.5) \cdot 10^{-6}\,\mathrm{g \cdot cm^{-2}}$, we obtained densely packed monolayers of nanoparticles with SPAR bands in the visible range.

Layer thicknesses were controlled with a quartz sensor. The film structure was studied with the use of an atomic force microscope Solver P47-PRO in the semicontact mode. We used special supersharp cantilevers made of a diamond-like carbon and characterized by a probe curvature radius under 3 nm, a stiffness coefficient of 5.1 N/m, and a resonance frequency of 150 kHz.

Optical spectra were recorded by a Cary 500 spectrophotometer.

Results and Discussion

We fabricated and studied both S-PPP-Ag and S-Ag-PPP systems. The S-Ag-PPP nanostructures were densely packed monolayers of silver nanoparticles evaporated on a substrate and covered by a thin layer of the polymer. The conjugated polymer was synthesized from benzol. The refractive index of polyparaphenylene films with thicknesses about tens of nanometers prepared with the use of this procedure was found to be about 1.75 [3]. In our case, the polymer films had a very small thickness (approximately 5 nm) that allows assuming a lower value of its refractive index (about 1.7). The S-PPP-Ag nanostructures were prepared by the evaporation, firstly, of a thin polyparaphenylene film on the substrate and then a densely packed monolayer of silver nanoparticles.

As the samples for comparison, we also prepared and tested the S-Ag nanostructures with various surface densities of the metal.

Figure 1a illustrates the surface images made with the use of an atomic force microscope for a silver monolayer with a metal surface concentration of $5.5 \cdot 10^{-6}\,\mathrm{g \cdot cm^{-2}}$. This figure shows that a metal film is nanostructured and characterized by the extremely high packing density of nanoparticles. From the size distribution histogram of Ag-islands given in Fig. 1b, one can see that the nanoparticle mean size is $\sim$13 nm. At the same time, there are large quantities both of fine nanoparticles (5–10 nm) and relatively large nanoparticles (with sizes of 20 nm).

Figure 2a shows the AFM-image of the same monolayer covered by the PPP film with a thickness of 5 nm. As one can see, the PPP coating leads to the strong smoothing of the two-layer nanostructure surface in the vertical direction. The profile of a sample section along the marked line demonstrates height differences of the S-Ag-PPP nanostructure surface (Fig. 2b). As is evident, the mean size of roughnesses is less than 1 nm. This means that the PPP evaporation on the Ag nanoparticle monolayer results in the interparticle space filling by the evaporated material.

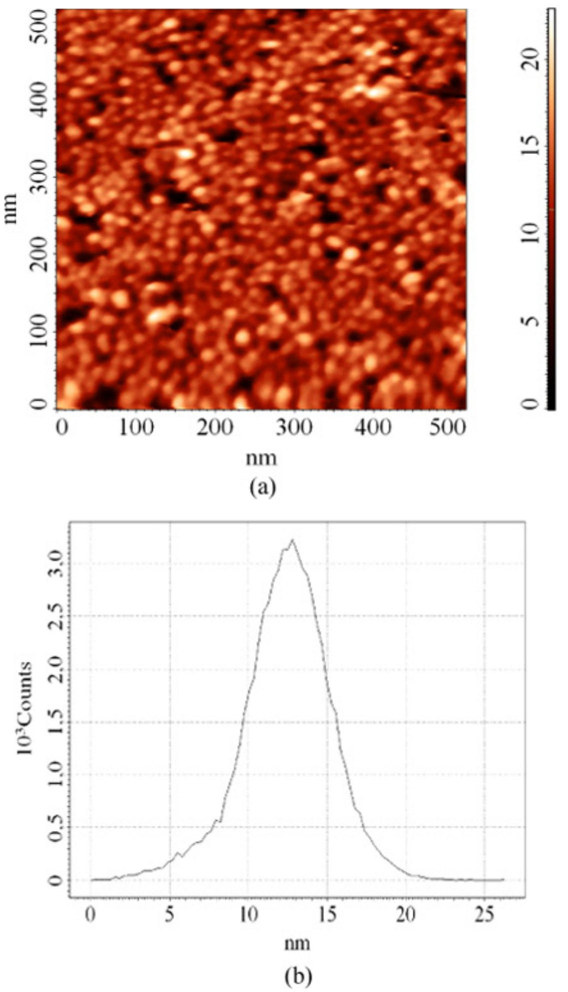

(a)

(b)

Figure 1. AFM-image (a) and the histogram of the nanoparticle size distribution (b) for the Ag nanoparticles monolayer with a metal surface density of $5.5 \cdot 10^{-6}\,\mathrm{g} \cdot \mathrm{cm}^{-2}$.

Figure 3 (curve 1) demonstrates the optical density spectra of the Ag monolayer shown in Figure 1. This nanostructure SPAR band covers practically the entire visible range of the spectrum and has maximum at 590 nm. The PPP film plating leads to a SPAR maximum long-wave shift up to 620 nm (Figure 3, curve 2). The shift value reaches 30 nm. A transmission decrease in the short-wave region $\lambda < 400\,\mathrm{nm}$ is related to the PPP absorption.

The PPP film with the same thickness of 5 nm was also applied on Ag monolayers with a metal density equal approximately to $1.7 \times 10^{-6}\,\mathrm{g} \cdot \mathrm{cm}^{-2}$. In this case, the mean size of Ag nanoparticles was 3–5 nm, and the overlapping factor equal to the ratio of all particle cross-sections to the sample cross-section was ~0.4. In Figure 4, one can observe the same long-wave shift of 30 nm between the SPAR maximum of the Ag monolayer (curve 1) and that of the S-Ag-PPP nanostructure (curve 2).

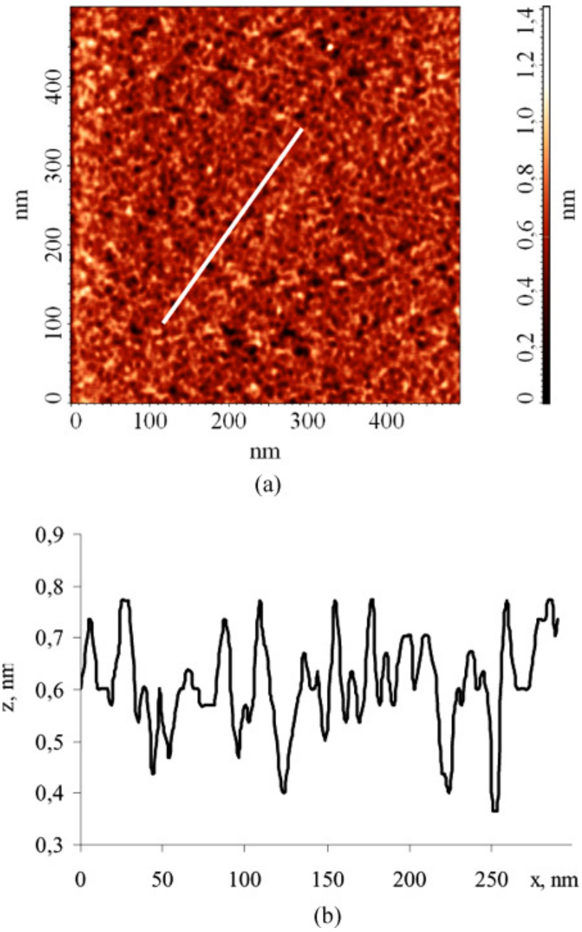

Figure 2. AFM-image of the S-Ag-PPP nanostructure surface (a) and a profile of the sample section along the marked line (b).

Thus, we have found that the thermal evaporation of a thin PPP film on monolayers with various surface densities of silver nanoparticles results in the SPAR maximum red shift of 30 nm. Now we will try to make clear the reasons for this effect.

In order to regard the SPAR maximum spectral position, one needs to consider three main circumstances. First of all, it is worth to note that, for the densely packed monolayers, the SPAR spectral position is strongly dependent on the electrodynamic coupling between metal nanoparticles situated closely to one another [4,5]. The close packing of nanoparticles results in a collective plasmon resonance generation. One of the main parameters that specifies the SPAR spectral position for the densely packed systems is the overlapping factor η. As the overlapping factor increases, the electrodynamic coupling enhances, and the collective SPAR band shifts to the long-wave range. For example, one can find this effect, by comparing the SPAR spectral positions for the S-Ag systems in Figures 3 and 4.

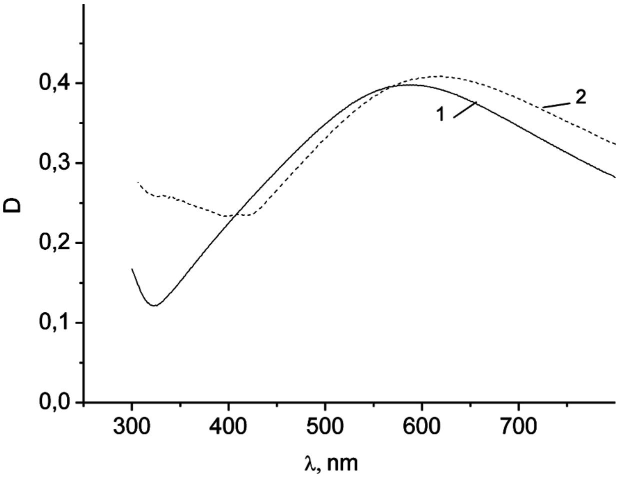

Figure 3. Optical density spectra for the Ag nanoparticles monolayer with a metal surface density of $5.5 \cdot 10^{-6}\,\mathrm{g \cdot cm^{-2}}$ (1) and for the same Ag nanoparticles monolayer covered by the PPP film (2) on the quartz substrate.

The second reason is the substrate effect. In order to clarify the influence of this factor, it seems appropriate to consider the case where the matrix refractive index changes in a wide range including both values which are less than the substrate refractive index and values which are higher than this magnitude.

Earlier, it was shown that a silver nanoparticle monolayer placed onto the matrix with the refractive index n_m less than 1.5 is characterized by a shorter SPAR maximum wavelength than a monolayer with the same microstructural parameters placed on the glass or quartz substrates and free of a matrix [6,7]. It was proposed to explain this fact with regard for a change of an inhomogeneous field near the

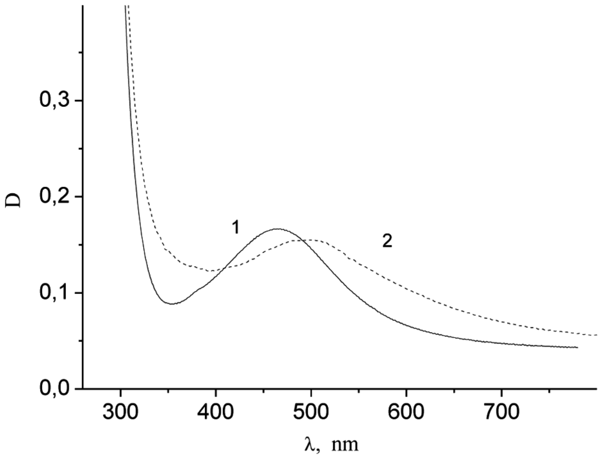

Figure 4. Optical density spectra for the Ag nanoparticles monolayer with a metal surface density of $1.7 \cdot 10^{-6}\,\mathrm{g \cdot cm^{-2}}$ (1) and the same Ag nanoparticles monolayer covered by the PPP film (2) on the glass substrate.

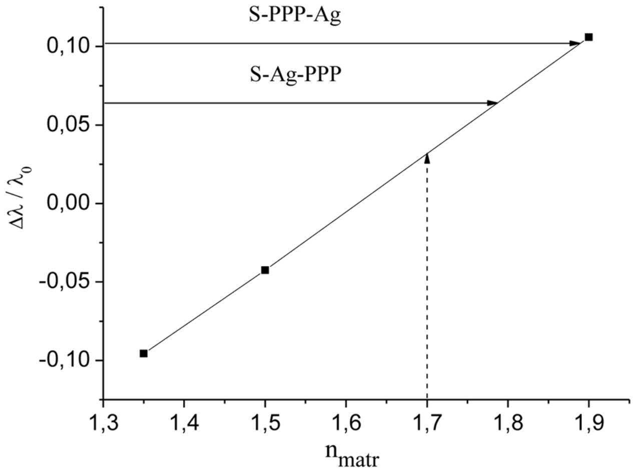

Figure 5. Sensitivity of the SPAR maximum spectral position to the matrix refractive indices for the densely packed monolayer consisted of silver nanoparticles with the mean size of 5 nm (λ_0 – wavelength of the SPAR maximum for the S-Ag nanostructure, $\Delta\lambda = \lambda_{\max} - \lambda_0$).

substrate surface, where metal nanoparticles are located. Actually, as n_m increases from 1 (air) to the substrate refractive index n_s (for glass and quartz substrates, n_s is about 1.5), the field near the substrate surface becomes more homogeneous, which may result in a decrease of the contribution of high-order multipoles and in a blue shift of the SPAR band as a result.

There is one more reason related to the so-called matrix effect due the Coulomb dynamic screening of electron collective oscillations into metal nanoparticles. The matrix screening enhances with increase in n_m and competes with a change of the inhomogeneous field, in which these nanoparticles are located. For instance, Figure 5 illustrates a sensitivity of the SPAR maximum to the matrix refractive indices for the densely packed monolayers consisting of silver nanoparticles with a mean size of about 5 nm and a metal surface density of about $2 \cdot 10^{-6}\,\text{g} \cdot \text{cm}^{-2}$. Together with polyparaphenylene, we also used matrices of Na_3AlF_6 ($n_m = 1.35$), KCl ($n_m = 1.5$), and SiO ($n_m = 1.9$). We note a long-wave shift of the SPAR maximum in the Na_3AlF_6-KCl-SiO series. The shift value is dependent on n_m linearly. The shift observed is essentially due a growth of the Coulomb dynamic screening. If the SPAR spectral position for the S-Ag-PPP nanostructure would be also governed only by the Coulomb dynamic screening, then it would be located near 485 nm ($\Delta\lambda/\lambda_0 = 0.064$). However, it is at 500 nm (see also Fig. 4). Furthermore, even larger are the SPAR shifts for the S-PPP - Ag nanostructures (see Fig. 5, $\Delta\lambda/\lambda_0 = 0.102$). Thus, the consideration we made allows assuming, together with the Coulomb dynamic screening, an additional reason for the red SPAR shift for two-layered polyparaphenylene-silver nanostructures. In our opinion, this may be the redistribution of the electron density in the polyparaphenylene-silver system accompanied by the electron doping of polyparaphenylene.

Taking the electronegativity (according to Pauling) for silver, hydrogen, and carbon (Ag – 1.9; H – 2.1; C – 2.5) into account [8], we may await that the Ag - PPP contact will simulate the electron transfer from Ag to PPP. It leads to a decrease of the silver nanoparticle plasma frequency which is proportional to the free electron number and stimulates a red shift of the SPAR.

Thus, the supersensitivity of the surface plasmon absorption resonances of Ag nanoparticles to the absence of a thin PPP layer may be caused by interactions of *sd*-hybridized conduction electrons of silver with π-electrons of PPP. From this point of view, we can also explain the fact that the magnitude of a red shift at the silver deposition on PPP is somewhat larger than that at the PPP deposition on silver (extinction maximum is shifted from 490 nm to 540 nm or by ~50 nm). The shift increase may be related to such a circumstance that, at the silver deposition on PPP, the larger number of metal atoms contacts with the surface of polymer, so the larger number of silver conduction electrons has a possibility for an active interaction with π-electrons of polyparaphenylene.

Conclusion

We have established the unusually large long-wave shift of the metal nanoparticle surface plasmon absorption resonance for the PPP-Ag and Ag-PPP nanostructures. Together with the Coulomb dynamic screening of collective electron oscillations in metal nanoparticles by the matrix material, the observed spectral shift may be connected with the PPP doping that leads to a change in metal nanoparticle electronic properties. The results obtained will be useful for developing the optimal variants of the conducting polymer activation that is important for widening the possibilities of their practical application. Because this effect is achieved with the use of thermal evaporation, it is easy to integrate the studied process in the planar technologies.

References

[1] Heeger, A. J. (2002). *Synth. Metals*, *123*, 23.

[2] Bohren, C., & Huffman, D. (1983). *Absorption and Scattering of Light by Small Particles*, Wiley: New York.

[3] Patent US No. 4588609.

[4] Kreibig, U., & Vollmer, M. (1995). *Optical Properties of Metal Clusters*, Springer: Berlin.

[5] Kachan, S. M., & Ponyavina, A. N. (2002). *J. Phys. Condens. Matter*, *14*, 103.

[6] Zamkovets, A. D., & Ponyavina, A. N. (2004). In: *Proceedings of II Seminar: "Nanotechnology and photonic crystalls"* (in Russian), Bauman MSTU: Kaluga-Moscow, p. 45.

[7] Zamkovets, A. D., Kachan, S. M., & Ponyavina, A. N. (2008). *J. Appl. Spectrosc.*, *75*, 588.

[8] Pauling, L. (1960). *The Nature of the Chemical Bond and the Structure of Molecules and Crystals: An Introduction to Modern Structural Chemistry*, Cornell Univ. Press: Ithaca, NY.